Synthetic GFP Chromophore and Control of Excited-State Proton Transfer in DNA: An Alternative Concept for Fluorescent DNA Labels with Large Apparent Stokes' Shifts

Ulrike Wenge, Hans-Achim Wagenknecht*[1]

University of Regensburg, Institute for Organic Chemistry, Universitätsstr. 31, 93053 Regensburg, Germany
Fax +49(941)9434617; E-mail: achim.wagenknecht@chemie.uni-regensburg.de

Received 22 September 2010; revised 17 November 2010

Abstract: Synthetic GFP-like chromophores bearing an *ortho*-phenol group instead of the *para*-phenol group of natural GFP can mimic the hydrogen bonding network in the protein by an intramolecular hydrogen bond to the imidazolone group. This hydrogen bond influences the excited state of the model by proton transfer (ESPT). The corresponding GFP model chromophore **1** was synthesized with an additional azide functionality that can be used to ligate it to acetylene-modified biomolecules by Cu(I)-catalyzed cycloaddition. The chromophore **1** was incorporated as a synthetic modification into oligonucleotides using a postsynthetic methodology and characterized within the DNA environment by optical spectroscopy. In order to elucidate the effect of DNA on ESPT a second GFP chromophore **2** was synthesized carrying a methyl group that prevents ESPT processes. It became evident that DNA is able to provide an artificial environment for the GFP chromophore that controls the photophysical property in such a way that nearly solely the ESPT-driven, red-shifted fluorescence is occurring. The apparent Stokes' shift is larger than 200 nm (9000 cm^{-1}). Moreover, the comparison with the methylated chromophore **2** in DNA elucidates that DNA increases the fluorescence intensity of both GFP models presumably by restricting the conformational flexibility. Although the observable quantum yields are too low to consider the fluorophore for any bioanalytical application, the combination of both effects, red-shifted ESPT-controlled fluorescence with large apparent Stokes' shifts and increase of intensity by restricting of internal conversion, provides an important concept for the design of fluorescent labels for DNA and RNA.

Key words: cyanine, fluorescence, green fluorescent protein, oligonucleotide, proton transfer

Green fluorescent proteins (GFPs) have been widely applied as fluorescent labels for bioanalytical applications and cell biology, especially live cell imaging.[2–6] There is continuous effort to further develop GFPs and GFP variants with enhanced brightness and with altered excitation as well as emission wavelengths, respectively.[5,6] GFP as a fluorescent marker is particularly useful since the chromophore is formed by a sequence of internal reactions that do not require a cofactor. The GFP chromophore consists of a *p*-hydroxybenzylidene-imidazol-5-one group and is formed via a posttranslational cyclization of a Ser-Tyr-Gly tripeptide followed by 1,2-dehydrogenation (autooxidation) of the Tyr moiety.[7] The unique and remarkable photophysical properties of the GFP chromophore and its variants are the result of different types of interactions between the mature GFP chromophore and its immediate protein neighborhood. The two parts of the π-conjugated system, the phenol, and the imidazolone group, are interconnected by a methine bridge, which is known from synthetic fluorescent cyanine dyes. Due to the conformational flexibility the fluorescence of the isolated GFP dye in solution is quenched by radiationless internal conversion, similar to other cyanine dyes, for instance thiazole orange. The GFP chromophore inside the protein is buried deeply in a rigid cylinder of β-sheets, which restricts the conformational flexibility, and thus suppresses the fast depopulation of the excited state by internal conversion.[8] On the other hand, the hydrogen bonding network of the GFP chromophore in the protein environment promotes an excited state proton transfer (ESPT) resulting in a very effective and intense anion fluorescence.[9] The two visible absorption bands at 390–400 nm (A band) and 470–480 nm (B band) have been attributed to the protonated and deprotonated state of this chromophore.[4,9,10] Excitation of the B band does not show unusual photophysical behavior. However, excitation of the predominant A band would normally emit blue light, but in fact emits green light. Upon photoexcitation the pK_a of the neutral chromophore changes from a typical phenolic value to near zero thus becoming a strong acid. Subsequent proton transfer through a preorganized hydrogen-bonding network rapidly generates the excited state anion with green fluorescence. The GFP chromophore demonstrates clearly that ESPT can be an extremely useful concept for the development of synthetic bioanalytical tools and probes. Hence, studies on synthetic GFP analogues are valuable and highly important not only for the understanding of the photophysical details of the natural chromophore inside the protein but also for designing and developing new and powerful synthetic fluorescent bioprobes.[11–16]

Synthetic GFP-like chromophores such as **1** bear an *ortho*-phenol group instead of the *para*-phenol group of natural GFP and thus can mimic the hydrogen bonding network of the protein by an intramolecular hydrogen bonding to the imidazolone group.[14] As a result, it is reported that a strongly enhanced fluorescence is observed for this isolated synthetic chromophore. Other studies have shown that encapsulation of the GFP chromophore[17] or synthetic incorporation into linear alaninyl peptide nucleic acids[18] can enhance the fluorescence quite signifi-

SYNTHESIS 2011, No. 3, pp 0502–0508
Advanced online publication: 10.01.2011
DOI: 10.1055/s-0030-1258400; Art ID: T19110SS
© Georg Thieme Verlag Stuttgart · New York

Downloaded by: University of Liverpool. Copyrighted material.

cantly. These examples indicate clearly that ESPT-controlled fluorescence becomes an increasingly important concept for the design of synthetic fluorophores as bioprobes with large apparent Stokes' shifts. To our knowledge, the concept of ESPT has not yet been applied for the development of fluorescent labels for DNA or RNA. Large Stokes' shifts are important to prevent artifacts in the fluorescent readout that are caused by scattering of the excitation light. Recently, we demonstrated the fluorescent labeling of DNA with so-called MegaStokes dyes that combine to FRET pairs with apparent Stokes' shifts of approximately 200 nm.[19] Herein, we present the principal achievement of large apparent Stokes' shifts by ESPT using a single fluorophore, the synthetic GFP model chromophore **1** (Scheme 1). In order to explore the potential of ESPT-controlled emission in DNA we chose the GFP chromophore due its well-characterized optical properties and photophysical behavior. In principle, double helical DNA should provide an artificial environment with stacking interactions and a hydrogen-bond network for the GFP chromophore. These structural features of DNA could represent a basis to modulate the GFP fluorescence by controlling both the rapid internal conversion due to restricted conformational flexibility and the ESPT by hydrogen bonds. We present herein a synthetic route to incorporate the GFP model chromophore **1** as a fluorescent modification into oligonucleotides using a postsynthetic methodology and the optical characterization of the GFP chromophore model within the DNA environment. In order to elucidate the effect of DNA on ESPT the GFP chromophore **2** was synthesized carrying a methyl group that prevents ESPT processes.

Both chromophores are equipped synthetically with an azide functionality. Among the various possible reactions for postsynthetic modifications,[20] the copper-catalyzed 1,3-dipolar cycloaddition between azides and terminal alkynes,[21] one of the so-called 'click'-type ligations,[22] ensures an easy access to covalent modifications of oligonucleotides. This fast, high yielding and biocompatible reaction does not interfere with other naturally occurring reactive sites (bioorthogonality).[23] This methodology is particularly suitable for fluorophores and other modification that would not be stable under the typical conditions of DNA preparation and workup. Accordingly, we recently reported about the single labeling of oligonucleotides with a coumarin dye and with MegaStokes dyes via the 'click'-type chemistry.[19,24] The dyes were ligated to a propargyl group that was attached to the 2′-OH function of the ribofuranoside part of uridine.[25] With respect to the acid sensitivity of **1** and **2** we applied this postsynthetic methodology to modify covalently DNA with the GFP chromophore.

The synthesis of the azides **1** and **2** started with the established Erlenmeyer azlactone synthesis.[26] The azlactone **5** was obtained from the starting materials **3** and **4** in good yield of 60% due to the methylated hydroxy function of the salicylic aldehyde **3** (Scheme 1). A free hydroxy group led mainly to coumarin derivatives. A C2 linker function

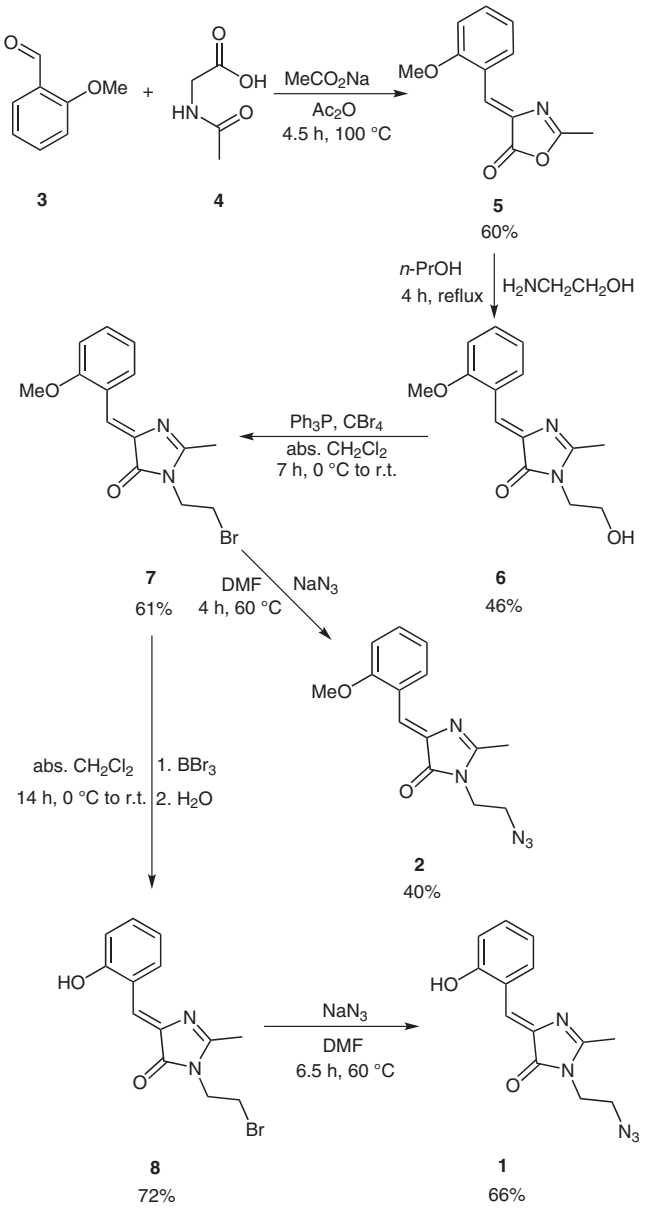

Scheme 1 Synthesis of the azides **1** and **2**

was attached to **5** via a one-pot ester cleavage and amide formation with ethanolamine.[27] Subsequently, the hydroxy group of the linker of **6** needs to be converted into a good leaving group. The Appel reaction generated the bromide **7**,[28] which was directly converted into the azide **2** by treatment with sodium azide in DMF.[29] Alternatively, the methylated hydroxy group of **7** can be deprotected by a standard procedure using boron tribromide at low temperature.[14] The deprotected chromophore **8** can then be converted into the azide **1**, again by treatment with sodium azide in DMF (Scheme 1). It is important to note that the azide formation must be the last step of the multistep synthesis, otherwise this functional group generates substantial amounts of side products during the remaining reactions. This was also the reason why the standard-type activation of the hydroxy group of the short linker in **6** by tosylation or mesylation[29] failed.

Downloaded by: University of Liverpool. Copyrighted material.

Before incorporating the GFP chromophores **1** and **2** into DNA we characterized their optical properties in aqueous buffer solution (Figure 1). At neutral pH, the chromophore **1** shows a broad absorption band with a maximum at 376 nm that stands in agreement with the published results.[14] The fluorescence spectra of **1** exhibit dual emission with peaks at 501 nm and at 596 nm. According to the literature, the latter band can be assigned to the emission that originates from an intramolecular ESPT state of the chromophore.[14] Interestingly, the published spectra of *o*-hydroxylated, synthetic GFP chromophores in an organic solvent (cyclohexane) show pure ESPT-driven fluorescence at 605 nm. The coexistence of both emissions (501 and 596 nm) in buffer as the solvent can be explained by incomplete intramolecular hydrogen bonding in water probably due to alternative hydrogen bonding possibilities with solvent molecules. If the ESPT is blocked by methylation of the hydroxyl group – see GFP chromophore **2** – the fluorescence is solely observable at 478 nm. On the other hand, ESPT fluorescence can be simulated by elevating the pH value of the aqueous solution to 13. The deprotonated phenolic function of the GFP chromophore **1** shifts the absorption to 448 nm and the emission to 595 nm. The latter emission occurs at a similar wavelength as the ESPT-driven emission of **1** at pH 7, but with significantly stronger intensity (Table 1).

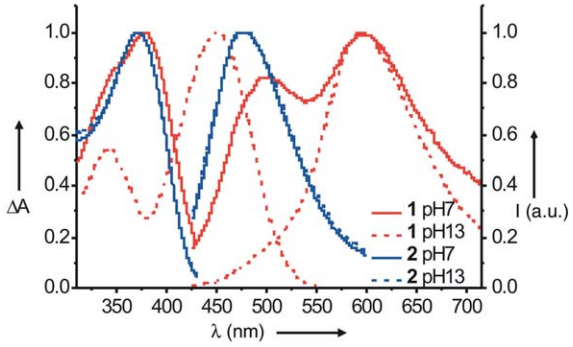

Figure 1 Normalized UV/Vis absorption and fluorescence of the synthetic GFP chromophores **1** and **2** (100 μM) in Na-P_i (sodium phosphate) buffer at pH 7 or pH 13, excitation at 400 nm

The ethynyl-modified oligonucleotides were presynthesized according to the literature procedure,[24,25] reacted with the azides **1** or **2**, respectively, according to our 'click'-type ligation protocol, worked up, purified, and identified according to the literature.[24] The two representative double strands that were synthesized expose the GFP chromophore **1** to two different variations in the sequential neighborhood: (i) The chromophore was placed either in a T-A (**DNA1Y**) or G-C base pair environment (**DNA2Y**). (ii) Within each duplex set, the base opposite to the GFP chromophore site was varied (**Y** = A, T, C or G). The methylated chromophore **2** was incorporated into duplex set **DNA3Y** that has identical sequences as **DNA1Y** to elucidate the ESPT effect (Figure 2).

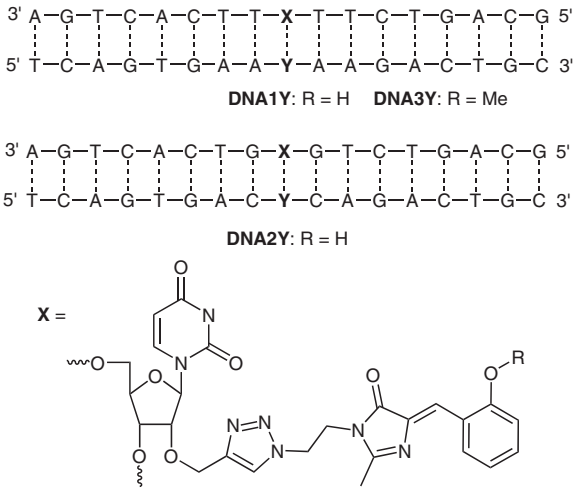

Figure 2 Sequences of **DNA1Y** and **DNA2Y**, modified with GFP chromophore **1**, and **DNA3Y** modified with the methylated GFP chromophore **2** (each duplex set with **Y** = A, T, C, or G)

The melting temperatures (T_m) revealed that especially purines opposite the GFP chromophore cause destabilization by –1.8 °C to –5.2 °C (Table 1). Based on our experience with other chromophores,[19,24] such values were expected. Interesting is the observation that the presence of T opposite to the chromophore **1** in **DNA1T** and **DNA2T** yields a clear stabilizing effect of +4.6 and +3.0 °C, respectively, although T forms a mismatch with the GFP chromophore modified uridine. This effect is diminished by methylation of the chromophore hydroxy group (in **DNA3T**). The measured T_m differences are in the range of an additional hydrogen bond.[30] Hence, we propose that the chromophore arrangement in **DNA1T** and **DNA2T** allows an additional hydrogen bond between the phenolic hydroxy group of the chromophore and one of the carbonyl groups of the opposite T. This special structural scenario causes slightly changed optical properties as discussed below.

The following discussion of the optical properties is focused mainly on the two different structural effects how DNA potentially affects the GFP chromophore fluorescence: (i) the control of ESPT by hydrogen bonding and (ii) the control of the rapid internal conversion by less conformational flexibility. Interactions of the GFP chromophores, **1** and **2**, with the DNA base stack can be clearly seen by the bathochromic shift of both absorption and emission of a few nm. The base opposite to the GFP chromophore modification site has an additional influence on the optical properties. Especially with T at the opposite position (**DNA1T** and **DNA2T**) both absorption and fluorescence are additionally red-shifted by up to 10 nm. These observations go along with the enhanced thermal stability of these two duplexes.

Except for the small bathochromic shifts, the absorption properties of **DNA1Y** and **DNA2Y** are very similar to the absorption of the isolated chromophore **1** whereas the fluorescence spectra display remarkable differences (Figure 3). Both emission bands (ESPT-controlled and

Downloaded by: University of Liverpool. Copyrighted material.

Table 1 Melting Temperatures, Optical Properties, and Quantum Yields of **1**, **2**, and **DNA1Y-3Y**

Product	T_m (°C)	ΔT_m (°C)[a]	λ_{abs} (nm)	λ_{em} (nm)	$\Delta\lambda$ (nm)	Φ_F (10^{-3})
1	–	–	376	501/596	125/220	0.19
1 (pH 13)	–	–	448	595	147	0.67
2	–	–	370	478	108	0.14
DNA1A	58.3	–4.2	393	609	216	4.3
DNA1G	53.0	–2.0	396	611	215	–[b]
DNA1T	57.8	+4.6	403	617	214	–[b]
DNA1C	52.5	–0.3	397	609	212	–[b]
DNA2A	66.0	–2.0	393	610	217	1.9
DNA2G	62.0	–1.8	396	607	211	–[b]
DNA2T	63.3	+3.0	400	613	213	–[b]
DNA2C	60.5	+2.2	397	607	210	–[b]
DNA3A	57.3	–5.2	382	460	78	2.7
DNA3G	51.7	–3.3	386	458	72	–[b]
DNA3T	53.5	+0.3	389	467	78	–[b]
DNA3C	50.5	–2.3	389	467	78	–[b]

[a] Compared to a completely unmodified DNA duplex.
[b] Not determined.

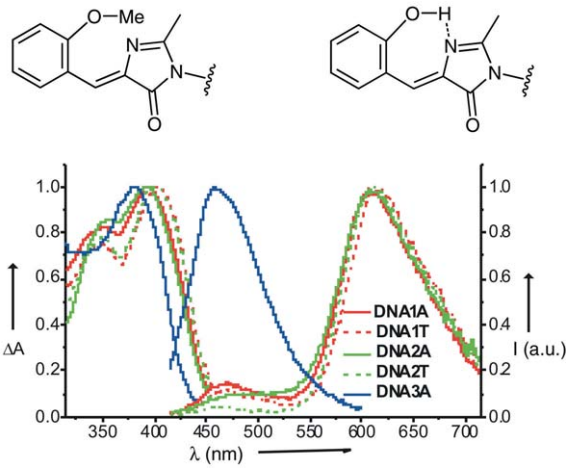

Figure 3 Normalized UV/Vis absorption and fluorescence of **DNA1A, DNA1T**, **DNA2A, DNA2T**, and **DNA3A** (2.5 μM) in Na-P_i buffer at pH 7, excitation at 400 nm

non-ESPT-controlled) of the isolated chromophore **1** at pH 7 show almost equal intensities (as discussed above). In contrast, the fluorescence spectra of all duplexes within the set **DNA1Y** are dominated by the red-shifted, ESPT-controlled band. The observable effect is even more pronounced in the set **DNA2Y**; here the non-ESPT-controlled band has nearly vanished. This is a remarkable result, since it shows that DNA is able to provide an environment that is similar to an organic solvent. That means that DNA protects the chromophore from hydrogen bonding with the surrounding water and enforces the presence of the intramolecular hydrogen bond in the chromophore.

Measurements of the quantum yields of the isolated chromophore are vey low (Φ_F $0.19 \cdot 10^{-3}$), but enhanced by factor of more than 20 inside the duplex **DNA1A** and 10 in **DNA2A**. In order to avoid misunderstandings it is important to mention here, that the quantum yields in DNA, although enhanced, are still far too low to apply similar GFP-modified oligonucleotides in any imaging or bioanalytical application.

With respect to these results, the duplexes of set **DNA3Y** represent important controls by two different means. Firstly, the strongly enhanced red-shifted fluorescence at ~600 nm is completely absent due to the presence of the methyl group as a blocker for ESPT. Secondly and more importantly, the fluorescence of **DNA3A** exhibits a nearly 20-fold increase of the intensity compared to the isolated chromophore **2**, a similar enhancement as observed with **DNA1A**. Hence, the fluorescence enhancement cannot be attributed to the ESPT but to the reduced conformational flexibility and decreased radiationless decay by rapid internal conversion. Of course, we do not know if these effects are caused by intercalation of the GFP chromophore (similar to ethidium bromide) or just by groove binding (similar to cyanine dyes). Nevertheless, it is remarkable to note that DNA is able (i) not only to control the ESPT for increasing the apparent Stokes' shift (of **1**) but (ii) also to increase the fluorescence intensity by restricting the conformational rotation freedom around the methine bridge of synthetic GFP chromophores (in **1** and **2**). The *combination* of both effects provides a promising concept to achieve fluorescent labels for nucleic acids with large apparent Stokes' shifts.

In conclusion, a synthetic route has been worked out to prepare and equip the GFP model chromophores **1** and **2** with an azide group for 'click'-type conjugation to biomolecules. The synthetic GFP-like chromophore **1** bears an *o*-phenol group instead of the *p*-phenol group of natural GFP and thus can mimic the hydrogen bond network inside DNA by an intramolecular hydrogen bond to the imidazolone group. At neutral pH, the spectra of **1** show dual emission, the 'normal' and the ESPT-driven, red-shifted fluorescence. Once incorporated into DNA as a 2′-modification using a postsynthetic strategy, the fluorescence spectra of all double strands within the set **DNA1Y** are dominated by the red-shifted, ESPT-controlled band. Obviously, DNA is similar to an organic solvent with respect to providing an artificial environment for the GFP chromophore that enforces the presence of the intramolecular hydrogen bond in the chromophore and controls its photophysical property in such a way that nearly solely the ESPT-driven, red-shifted fluorescence is occurring. The apparent Stokes' shift of ca. 210 nm (9000 cm^{-1}) is remarkably high for a single fluorophore and separates nicely excitation from emission light, a desirable feature for many imaging and bioanalytical applications. Moreover, the comparison with the methylated chromophore **2** in

Downloaded by: University of Liverpool. Copyrighted material.

DNA makes clear that the presence of DNA increases the fluorescence intensity by restricting the conformational flexibility in the GFP chromophore. The latter effect is well known from various other cyanine dyes. The observable quantum yields of the GFP chromophore in DNA are too small to be relevant for applications. However, the combination of both effects, red-shifted ESPT-controlled fluorescence with large apparent Stokes' shifts and increase of intensity by restricting of internal conversion is very attractive for the design of new and powerful fluorescent labels for DNA and RNA. Herein we evidenced these principles for the well-known GFP chromophore attached to DNA. Future work will show how this concept can be transferred to other fluorophores with higher quantum yields.

TLC was carried out with silica gel 60 on aluminum foil (Merck). ^{1}H and ^{13}C spectra were recorded on Bruker Avance 300 and 400 instruments; chemical shifts (δ) are referred to residual protonated solvent. HRMS spectra were recorded on a Finnigan MAT 95 spectrometer. ESI-MS spectra were recorded on a ThermoQuest Finnigan TSQ 7000 spectrometer. CI-MS spectra were recorded on a Finnigan MAT SSQ710 spectrometer. Absorption measurements were carried out on Cary 100 (Varian) spectrometer at 20 °C. Fluorescence measurements were performed on Fluoromax-3 (Horiba Jobin Yvon) spectrometer at 20 °C. The quantum yields of the isolated model compounds **1** and **2** were measured with perylene as standard. The intensity of the excitation light had to be reduced to 0.1% by applying a neutral glass filter. In the case of modified DNA, the quantum yields were measured with zinc(II)-5,10,15,20-tetraphenyl-21*H*,23*H*-porphyrinate as standard, and the intensity of the excitation light had to be reduced to 26.4%.

4-(2-Methoxybenzylidene)-2-methyloxazol-5(4*H*)-one (5)

o-Anisaldehyde (**3**; 14.0 mL, 15.8 g, 116 mmol), *N*-acetylglycine (**4**; 14.0 g, 120 mmol, 1.03 equiv), and anhyd NaOAc (10.7 g, 130 mmol, 1.12 equiv) in Ac_2O (47 mL, 51.0 g, 500 mmol) were stirred at 100 °C for 4.5 h. The mixture was allowed to cool down to r.t. Ice water (50 mL) was added. The resulting precipitate was collected by filtration, washed with ice water, and dried in vacuum; yield: 15.2 g (60%); yellow solid.

^{1}H NMR (300 MHz, $CDCl_3$): δ = 2.35 (s, 3 H, CH_3C), 3.85 (s, 3 H, CH_3O), 6.87 (d, *J* = 8.5 Hz, 1 H, ArH), 6.99 (t, *J* = 7.6 Hz, 1 H, ArH), 7.32–7.38 (m, 1 H, ArH), 7.71 (s, 1 H, HC=C), 8.56–8.60 (m, 1 H, ArH).

^{13}C NMR (100 MHz, $CDCl_3$): δ = 15.6 (*C*H_3C), 55.6 (CH_3O), 110.7 (ArCH), 120.9 (ArCH), 122.2 (Ar*C*C), 125.7 (H*C*=C), 131.8 (HC=*C*), 132.5 (ArCH), 132.8 (ArCH), 159.1 (C–O), 165.5 (C=N), 168.0 (C=O).

CI-MS: *m*/*z* (%) = 217.1 (29, [M$^+$]).

HRMS (EI-MS): *m*/*z* [M$^+$] calcd for $C_{12}H_{11}NO_3$: 217.0739; found: 217.0740.

1-(2-Hydroxyethyl)-4-(2-methoxybenzylidene)-2-methyl-1*H*-imidazol-5(4*H*)-one (6)

To a solution of **5** (5.00 g, 23 mmol) in anhyd *n*-propanol (23 mL), ethanolamine (1.52 mL, 1.55 g, 25 mmol, 1.10 equiv) was added. The reaction mixture was heated under reflux for 5 h. The solvent was evaporated and the residue was purified by recrystallization from pentanol–Et_2O mixture, yield: 2.78 g (46%); yellow solid.

^{1}H NMR (300 MHz, CD_3OD): δ = 2.44 (s, 3 H, CH_3C), 3.73 (m, 4 H, CH_2), 3.91 (s, 3 H, CH_3O), 6.98–7.04 (m, 2 H, ArH), 7.36–7.42 (m, 1 H, ArH), 7.57 (s, 1 H, HC=C), 8.55–8.58 (m, 1 H, ArH).

^{13}C NMR (75 MHz, CD_3OD): δ = 15.8 (*C*H_3C), 44.4 (CH_2), 56.3 (CH_3O), 60.7 (CH_2), 111.9 (ArCH), 121.7 (ArCH), 122.3 (H*C*=C), 124.0 (Ar*C*C), 133.3 (ArCH), 133.9 (ArCH), 139.0 (HC=*C*), 160.6 (C–O), 165.5 (C=N), 172.4 (C=O).

ESI-MS: *m*/*z* (%) = 261.0 (100, [M + H]$^+$).

HRMS (EI-MS): *m*/*z* [M$^+$] calcd for $C_{14}H_{16}N_2O_3$: 260.1161; found: 260.1161.

1-(2-Bromoethyl)-4-(2-methoxybenzylidene)-2-methyl-1*H*-imidazol-5(4*H*)-one (7)

Compound **6** (600 mg, 2 mmol) was dissolved in anhyd CH_2Cl_2 (23 mL) under N_2 atmosphere. First, Ph_3P (670 mg, 3 mmol, 1.10 equiv) was added at 0 °C, then, after 10 min, CBr_4 (920 mg, 3 mmol, 1.20 equiv) was added. The mixture was stirred at r.t. for 7 h. Then additional Ph_3P (670 mg, 3 mmol, 1.10 equiv) and CBr_4 (920 mg, 3 mmol, 1.20 equiv) were added. After 1.5 h, the solvent was removed under reduced pressure, and the residue was purified by flash chromatography with CH_2Cl_2–acetone (5:1); yield: 460 mg (61%); orange solid; R_f = 0.86 (CH_2Cl_2–acetone, 10:1).

^{1}H NMR (300 MHz, $CDCl_3$): δ = 2.41, (s, 3 H, CH_3C), 3.56 (t, *J* = 6.3 Hz, 2 H, CH_2), 3.84 (s, 3 H, CH_3O), 3.97 (t, *J* = 6.3 Hz, 2 H, CH_2), 6.85 (d, *J* = 8.4 Hz, 1 H, ArH), 6.99 (t, *J* = 7.7 Hz, 1 H, ArH), 7.28–7.34 (m, 1 H, ArH), 7.66 (s, 1 H, HC=C), 8.67–8.70 (m, 1 H, ArH).

^{13}C NMR (75 MHz, $CDCl_3$): δ = 16.0 (*C*H_3C), 29.0 (CH_2), 42.6 (CH_2), 55.6 (CH_3O), 110.6 (ArCH), 120.9 (ArCH), 122.2 (H*C*=C), 123.0 (Ar*C*C), 132.0 (ArCH), 132.9 (ArCH), 137.4 (HC=*C*), 159.2 (C–O), 161.0 (C=N), 170.5 (C=O).

ESI-MS: *m*/*z* (%) = 324.9 (100, [M + H]$^+$).

HRMS (EI-MS): *m*/*z* [M$^+$] calcd for $C_{14}H_{15}BrN_2O_2$: 322.0317; found: 322.0316.

1-(2-Azidoethyl)-4-(2-methoxybenzylidene)-2-methyl-1*H*-imidazol-5(4*H*)-one (2)

Compound **7** (100 mg, 0.3 mmol) and NaN_3 (200 mg, 3.1 mmol, 10.00 equiv) were dissolved in DMF (3 mL) and stirred for 3 h at 60 °C. The suspension was mixed with H_2O (4 mL) and extracted with CH_2Cl_2 (3 × 3 mL). The combined organic phases were washed with brine (3 × 15 mL) and dried (Na_2SO_4). The solvent was evaporated and the residue was purified by flash chromatography using CH_2Cl_2–acetone (400:1) as eluent; yield: 35 mg (40%); yellow solid, R_f = 0.52 (CH_2Cl_2–acetone, 50:1).

^{1}H NMR (300 MHz, CD_3OD): δ = 2.42 (s, 3 H, CH_3C), 3.61 (t, *J* = 5.5 Hz, 2 H, CH_2), 3.74 (t, *J* = 5.5 Hz, 2 H, CH_2), 3.88 (s, 3 H CH_3O), 6.89 (d, *J* = 8.3 Hz, 1 H, ArH), 7.03 (t, *J* = 7.6 Hz, 1 H, ArH), 7.32–7.38 (m, 1 H, ArH), 7.69 (s, 1 H, HC=C), 8.71–8.74 (m, 1 H, ArH).

^{13}C NMR (75 MHz, CD_3OD): δ = 14.8 (*C*H_3C), 39.1 (CH_2), 48.8 (CH_2), 54.3 (CH_3O), 109.6 (ArCH), 119.9 (ArCH), 121.0 (H*C*=C), 122.0 (Ar*C*C), 130.9 (ArCH), 131.9 (ArCH), 136.5 (HC=*C*), 158.1 (C–O), 160.3 (C=N), 169.6 (C=O).

ESI-MS: *m*/*z* (%) = 286.0 (100, [M + H]$^+$).

HRMS (EI-MS): *m*/*z* [M$^+$] calcd for $C_{14}H_{15}N_5O_2$: 285.1226; found: 285.1223.

1-(2-Bromoethyl)-4-(2-hydroxybenzylidene)-2-methyl-1*H*-imidazol-5(4*H*)-one (8)

Compound **7** (170 mg, 0.51 mmol) was dissolved in anhyd CH_2Cl_2 under N_2 atmosphere and cooled to 0 °C. A 1.0 M solution of BBr_3 in CH_2Cl_2 (0.54 mL, 1.06 equiv) was added dropwise over 15 min. After stirring overnight, H_2O (5 mL) was added and stirred for 0.5 h. The aqueous phase was extracted with CH_2Cl_2 (2 × 10 mL) The combined organic phases were dried (Na_2SO_4) and the solvent was

Downloaded by: University of Liverpool. Copyrighted material.

evaporated. The solid was purified by flash chromatography using CH_2Cl_2–acetone (50:1) as eluent; yield: 113 mg (72%); yellow solid; R_f = 0.68 (CH_2Cl_2–acetone, 50:1).

^{1}H NMR (300 MHz, $CDCl_3$): δ = 2.44 (s, 3 H, CH_3C), 3.60 (t, J = 6.1 Hz, 2 H, CH_2), 4.02 (t, J = 6.1 Hz, 2 H, CH_2), 6.80–6.85 (m, 1 H, ArH), 6.96 (d, J = 8.2 Hz, 1 H, ArH), 7.15 (s, 1 H, HC=C), 7.24–7.35 (m, 2 H, ArH).

^{13}C NMR (75 MHz, $CDCl_3$): δ = 15.6 (*C*H_3C), 29.8 (CH_2), 43.7 (CH_2), 119.2 (ArCH), 120.7 (ArCH), 121.1 (Ar*C*C), 129.2 (H*C*=C), 134.9 (ArCH), 135.0 (HC=*C*), 136.8 (ArCH), 159.6 (C=N), 160.9 (C–O), 170.1 (C=O).

ESI-MS: *m*/*z* (%) = 308.8 (100, $[M + H]^+$).

HRMS (EI-MS): *m*/*z* [M^+] calcd for $C_{13}H_{13}BrN_2O_2$: 308.0161; found: 308.0163.

1-(2-Azidoethyl)-4-(2-hydroxybenzylidene)-2-methyl-1*H*-imidazol-5(4*H*)-one (1)

Compound **8** (40 mg, 0.14 mmol) and NaN_3 (93 mg, 1.42 mmol, 10.0 equiv) were dissolved in DMF (1.4 mL) and stirred for 4 h at 60 °C. The suspension was mixed with H_2O (2 mL) and extracted with CH_2Cl_2 (3 × 2 mL). The combined organic phases were washed with brine (2 × 10 mL) and dried (Na_2SO_4). The solvent was evaporated and the residue was purified by flash chromatography using CH_2Cl_2–acetone (50:1) as eluent; yield: 25 mg (66%); light yellow solid; R_f = 0.60 (CH_2Cl_2–acetone, 50:1).

^{1}H NMR (300 MHz, $CDCl_3$): δ = 2.41, (s, 3 H, CH_3C), 3.60–3.64 (m, 2 H, CH_2), 3.72–3.77 (m, 2 H, CH_2), 6.80–6.85 (m, 1 H, ArH), 6.92 (d, J = 8.0 Hz, 1 H, ArH), 7.15 (s, 1 H, HC=C), 7.24–7.35 (m, 2 H, ArH), 13.67 (s, 1 H, OH).

^{13}C NMR (100 MHz, $CDCl_3$): δ = 15.4 (*C*H_3C), 40.5 (CH_2), 49.6 (CH_2), 119.3 (ArCH), 119.5 (ArCH, Ar*C*C), 130.9 (H*C*=C), 132.2 (HC=*C*), 134.4 (ArCH), 136.5 (ArCH) 157.0 (C=N), 158.7 (C–O), 167.9 (C=O).

ESI-MS: *m*/*z* (%) = 271.9 (100, $[M + H]^+$).

HRMS (EI-MS): *m*/*z* [M^+] calcd for $C_{13}H_{13}N_5O_2$: 271.1069; found: 271.1069

Modified Oligonucleotides

Oligonucleotides were prepared on an Expedite 8909 Synthesizer from Applied Biosystems (ABI) using standard phosphoramidite chemistry. Reagents and controlled pore glass (CPG) (1 μmol) were purchased from Proligo. 5′-*O*-Dimethoxytrityl-N^3-pivaloyloxymethyl-2′-*O*-propargyluridine-3′-*O*-(2-cyanoethyl-*N*,*N*-diisopropyl-phosphoramidite was synthesized according to the literature procedure.[24] The concentration of the uridine building block was increased to 0.1 M. After preparation, the trityl-off oligonucleotides were cleaved from the resin and deprotected by treatment with concd NH_4OH at 50 °C for 15 h. The azide **1** or **2** (114 μL, 10 mM), Cu(I) (17 μL, 100 mM), TBTA (34 μL, 100 mM), each in DMSO–*t*-BuOH (3:1), and sodium ascorbate (25 μL, 400 mM) in H_2O were added to the oligonucleotide (1 μmol scale). The reaction mixture was vortexed, shaken overnight at r.t., and then evaporated to dryness using a speedvac. NaOAc (100 μL, 0.15 mmol) and EtOH (1 mL) were added, vortexed and frozen (–20 °C) overnight. The suspension was centrifuged (13 000 rpm, 15 min), and the supernatant removed. The pellet was dissolved in H_2O (500 μL). Prior to purification by HPLC, the DNA was desalted by NAP-5 column (GE Healthcare). The modified oligonucleotides were purified by HPLC on a semi-preparative RP-C18 column (300 Å, Supelco), using the following conditions: A) NH_4OAc buffer (50 mM, pH 6.5); B) MeCN, gradient 0–20% B over 45 min, flow rate 2.5 mL/min, UV/VIS detection at 260 nm and 378 nm. The modified oligonucleotides were lyophilized, identified by ESI mass spectrometry, and quantified by UV/Vis absorption using extinction coefficients of 2400 L/mol·cm for **1** and 3800 L/mol·cm for **2**, both at 260 nm. DNA duplexes are formed by heating in the presence of 1.2 equiv of the unmodified counterstrands at 90 °C for 10 min followed by slow cooling to r.t.

ESI-MS:

DNA1: *m*/*z* calcd for $C_{181}H_{225}N_{61}O_{107}P_{16}$: 5460.0 Da; found: 1365.0 $[M - 4 H]^{4-}$, 1820.3 $[M - 3 H]^{3-}$

DNA2: *m*/*z* calcd for $C_{181}H_{223}N_{67}O_{105}P_{16}$: 5510.0 Da; found: 1377.3 $[M - 4 H]^{4-}$, 1837.2 $[M - 3 H]^{3-}$

DNA3: *m*/*z* calcd for $C_{182}H_{227}N_{61}O_{107}P_{16}$: 5474.0 Da; found: 1368.4 $[M - 4 H]^{4-}$, 1825.0 $[M - 3 H]^{3-}$

Supporting Information for this article is available online at http://www.thieme-connect.com/ejournals/toc/synthesis.

Acknowledgment

Financial support is acknowledged from the University of Regensburg and the Deutsche Forschungsgemeinschaft.

References

(1) New address: Karlsruhe Institute of Technology, Institute for Organic Chemistry, Fritz-Haber-Weg 6, 76131 Karlsruhe, Germany; Fax: +49(721)60844825; e-mail: Wagenknecht@kit.edu.
(2) (a) Shimomura, O.; Johnson, F. H.; Saiga, Y. *J. Cell. Comp. Physiol.* **1962**, *59*, 223. (b) Shimomura, O. *Angew. Chem. Int. Ed.* **2009**, *48*, 5590.
(3) (a) Chalfie, M.; Tu, Y.; Euskirchen, G.; Ward, W. W.; Prasher, D. C. *Science* **1994**, *263*, 802. (b) Chalfie, M. *Angew. Chem. Int. Ed.* **2009**, *48*, 5603.
(4) (a) Heim, R.; Prasher, D. C.; Tsien, R. Y. *Proc. Natl. Acad. Sci. USA* **1994**, *91*, 12501. (b) Tsien, R. Y. *Angew. Chem. Int. Ed.* **2009**, *48*, 5612.
(5) See review: Zimmer, M. *Chem. Rev.* **2002**, *102*, 759.
(6) See reviews: (a) Remington, S. J. *Curr. Opin. Struct. Biol.* **2006**, *16*, 714. (b) Zhang, J.; Campbell, R. E.; Ting, A. Y.; Tsien, R. Y. *Nature Rev. Mol. Cell Biol.* **2002**, *3*, 906.
(7) (a) Prasher, D. C.; Eckenrode, V. K.; Ward, W. W.; Prendergast, F. G.; Cormier, M. J. *Gene* **1992**, *111*, 229. (b) Cody, C. W.; Prasher, D. C.; Westler, W. M.; Prendergast, F. G.; Ward, W. W. *Biochemistry* **1993**, *32*, 1212.
(8) Kummer, A. D.; Kompa, C.; Lossau, H.; Pöllinger-Dammer, F.; Michel-Beyerle, M. E.; Silva, C. M.; Bylina, E. J.; Coleman, W. J.; Yang, M. M.; Youvan, D. C. *Chem. Phys.* **1998**, *237*, 183.
(9) (a) Chattoraj, M.; King, B. A.; Bublitz, G. U.; Boxer, S. G. *Proc. Natl. Acad. Sci. USA* **1996**, *93*, 8362. (b) Brejc, K.; Sixma, T. K.; Kitts, P. A.; Kain, S. R.; Tsien, R. Y.; Ormö, M.; Remington, S. J. *Proc. Natl. Acad. Sci. USA* **1997**, *94*, 2306. (c) Palm, G. J.; Zdanov, A.; Gaitanaris, G. A.; Stauber, R.; Pavlakis, G. N. *Nat. Struct. Biol.* **1997**, *4*, 361.
(10) Niwa, H.; Inouye, S.; Hirano, T.; Matsuno, T.; Kojima, S.; Kubota, M.; Ohashi, M.; Tsuji, F. I. *Proc. Natl. Acad. Sci. USA* **1996**, *93*, 13617.
(11) Ai, H.-W.; Shaner, N. C.; Cheng, Z.; Tsien, R. Y.; Campbell, R. E. *Biochemistry* **2007**, *46*, 5904.
(12) Wu, L.; Burgess, K. *J. Am. Chem. Soc.* **2008**, *130*, 4089.
(13) Kojima, S.; Ohkawa, H.; Hirano, T.; Maki, S.; Niwa, H.; Ohashi, M.; Inouye, S.; Tsuji, F. I. *Tetrahedron Lett.* **1998**, *39*, 5239.

Downloaded by: University of Liverpool. Copyrighted material.

(14) Chen, K.-Y.; Cheng, Y.-M.; Lai, C.-H.; Hsu, C.-C.; Ho, M.-L.; Lee, G.-H.; Chou, P.-T. *J. Am. Chem. Soc.* **2007**, *129*, 4534.
(15) Kang, J.; Zhao, G.; Xu, J.; Yang, W. *Chem. Commun.* **2010**, *46*, 2868.
(16) Prüger, B.; Bach, T. *Synthesis* **2007**, 1103.
(17) Baldrige, A.; Samanta, S. R.; Jayaraj, N.; Ramamurthy, V.; Tolbert, L. M. *J. Am. Chem. Soc.* **2010**, *132*, 1498.
(18) Stafforst, T.; Diederichsen, U. *Eur. J. Org. Chem.* **2007**, 899.
(19) Ehrenschwender, T.; Varga, B. R.; Kele, P.; Wagenknecht, H.-W. *Chem. Asian J.* **2010**, *5*, 1761.
(20) See review: Weisbrod, S. H.; Marx, A. *Chem. Commun.* **2008**, 5675.
(21) Huisgen, R. *Angew. Chem. Int. Ed.* **1963**, *2*, 565.
(22) (a) Lewis, W. G.; Green, L. G.; Grynszpan, F.; Radic, Z.; Carlier, P. R.; Taylor, P.; Finn, M. G.; Sharpless, K. B. *Angew. Chem. Int. Ed.* **2002**, *41*, 1053. (b) Tornøe, C. W.; Christensen, C.; Meldal, M. *J. Org. Chem.* **2002**, *67*, 3057.
(23) See reviews: (a) Gramlich, P. M.; Wirges, C. T.; Manetto, A.; Carell, T. *Angew. Chem. Int. Ed.* **2008**, *47*, 8350. (b) El-Sagheer, A. H.; Brown, T. *Chem. Soc. Rev.* **2010**, *39*, 1388.
(24) Berndl, S.; Herzig, N.; Kele, P.; Lachmann, D.; Li, X.; Wolfbeis, O.; Wagenknecht, H.-A. *Bioconjugate Chem.* **2009**, *20*, 558.
(25) Grøtli, M.; Douglas, M.; Eritja, R.; Sproat, B. S. *Tetrahedron* **1998**, *54*, 5899.
(26) Bailly, F.; Maurin, C.; Teissier, E.; Vezin, H.; Cotelle, P. *Bioorg. Med. Chem.* **2004**, *12*, 5611.
(27) Shafi, P. M.; Basheer, P. A. M.; Jirovetz, L. *Asian J. Chem.* **2006**, *18*, 3188.
(28) See review: Appel, R. *Angew. Chem. Int. Ed.* **1975**, *14*, 801.
(29) See review: Bräse, S.; Gil, C.; Knepper, K.; Zimmermann, V. *Angew. Chem. Int. Ed.* **2005**, *44*, 5188.
(30) See review: Benner, S. A. *Acc. Chem. Res.* **2004**, *37*, 784.

Downloaded by: University of Liverpool. Copyrighted material.